Heliyon 5 (2019) e02752

Contents lists available at ScienceDirect

Heliyon

journal homepage: www.heliyon.com

Heliyon

Research article

# An experimental study of the influence of orientation on water condensation of a thermoelectric cooling heatsink

Carson T. Hand, Steffen Peuker *

*California Polytechnic State University, San Luis Obispo, CA, USA*

ARTICLE INFO

*Keywords:*
Mechanical engineering
Thermodynamics
Heat exchanger
Heat transfer
Thermoelectric cooler
Atmospheric water condensation
Atmospheric water harvesting
HVAC&R application

ABSTRACT

An experimental investigation of thermoelectric cooling using a Peltier element to dehumidify moist air under controlled, high relative humidity conditions has been conducted. The influence of the cold side heatsink orientation on the water collection rate was experimentally determined. One finned heatsink-fan combination was used on the heat rejection side. On the cold side flat plates, uncoated and Polytetrafluoroethylene (PTFE) coated, a fanned plate with four fins, and a heatsink having 15 fins were used. The PTFE coated plate showed up to a 30% higher water collection rate (expressed in L/kWh) compared to the uncoated flat plate that has the same surface area. Clearing the surfaces—removing all condensate every hour—increased the water collection rate by up to 18% for the flat plates. The finned heatsink and the PTFE coated flat plate were used for the orientation experiments. The finned heatsink was rotated from 0° to 90°, as well as tilted from 0° to 90° (vertical to horizontal). To investigate the effect of surface orientation on a single-side collection surface in isolation, the PTFE coated flat plate was tilted from 15° to 165° in 15° increments. The highest collection rates are found for a rotation angle of 60° and a tilted angle of 75° for the finned heatsink, 0.249 L/kWh and 0.221 L/kWh respectively. The highest measured collection rate for the PTFE coated plate is 0.319 L/kWh at an orientation of 15° from the horizontal. Experiments for the horizontal orientation of the finned heatsink show that once the spaces between the fins are completely filled with water the collection rate drops by an order of magnitude, from 0.203 L/kWh to 0.026 L/kWh. The experiments show that the orientation of a thermoelectric heatsink should be considered when optimizing the water collection rates under high humidity conditions for thermoelectric cooling heatsinks.

## 1. Introduction

Fins or extended surfaces are used in heat exchanger design to enhance the heat transfer, typically in liquid/two-phase fluid to gas heat exchangers to address the low values of heat-transfer coefficient on the gas side. Condensation occurs on the finned surface in applications when the finned surface temperature is below the saturation temperature of the gas in contact with the finned surface. Examples are heat exchangers used in industry to condense steam and air conditioning and refrigeration applications where water vapor from the air condenses on the heat exchanger surface. Condensation occurs either as film condensation or dropwise condensation. In most applications the objective is to have a high heat transfer rate and from this standpoint of view, dropwise condensation is preferred since dropwise condensation can result in more than 10 times higher heat transfer rates. However, sustained dropwise condensation is difficult to achieve as a result of the tendency for the droplets to convert to film condensation after some time [1]. The factors affecting condensation on finned surfaces include the geometry (shape) of the fins, the fin and surface material, and thermo-physical parameters. During condensation on finned surfaces heat and mass transfer take place simultaneously making the physics more complex. Studies focus on surface/droplet interactions and condensation [2], performance of heat exchangers under dehumidification conditions [3, 4], and the influence of heat transfer surfaces on wettability [5].

The presented study is an experimental investigation of a thermoelectric cooling heatsink used to dehumidify moist air under controlled, high relative humidity conditions. Studies have investigated the viability of using thermoelectric cooling to dehumidify or generate freshwater from the atmosphere. Milani et al. [6] investigated the feasibility of using thermoelectric coolers (TECs) devices in the dehumidification process to condense water vapor from the atmosphere. They concluded that the potential economic viability of TEC dehumidification systems may be further optimized by using larger cooling surfaces of hydrophilic dropwise condensation advocate materials and that advances in TECs design

* Corresponding author.
*E-mail address:* speuker@calpoly.edu (S. Peuker).

https://doi.org/10.1016/j.heliyon.2019.e02752
Received 18 July 2019; Received in revised form 25 September 2019; Accepted 25 October 2019

and development could further enhance the efficiency and productivity of dehumidification using TECs. A study by Liu et al. [7] was conducted with thermoelectric coolers (TECs). Liu et al. report that the TEC units reached steady state after 6–7 h and yielded an average of 11.2g water/hour with a power consumption of 52.3 W, using 2 TECs. They reported a maximum efficiency of 0.215 L/kWh. Vián et al. [8] used a numerical model to optimize a thermoelectric dehumidifier. The numerical model results overpredicted the water condensate flow rate by 36% compared to their experimental results. Their final optimized prototype achieved 0.404 L/kWh. Joshi et al. [9] experimentally investigated a portable thermoelectric fresh water generator using ten Peltier modules in a vertical array. The maximum efficiency of their prototype reached 0.178 L/kWh. Muñoz-García et al. [10] investigated the use of Peltier elements to condense water from the atmosphere for young tree irrigation. They performed their experiments under realistic ambient conditions and therefore their maximum relative humidity reported was around 70% relative humidity. The resulting efficiency of their device is around 0.1 L/kWh under these conditions. Eslami et al. [11] present a comprehensive thermodynamic analysis of water production from humid air using thermoelectric coolers (TECs). They report efficiencies ranging form 0.2–0.412 L/kWh for their optimized experimental system. Tan and Fok [12] built and tested an experimental prototype to study the application of using a thermoelectric cooler (TEC) to extract water from air. Under 77% relative humidity condition their prototype achieved an efficiency of 0.187 L/kWh.

The presented study focuses on the influence of the TEC heatsink orientation on the water collection rate which have not been reported previously for TEC application for atmospheric water harvesting. Rotation and tilting of the heatsink were experimentally investigated. The collection rates are expressed in volume of water per energy, L/kWh.

## 2. Materials and methods

The hot side heatsink chosen for this study is a typical cpu heatsink and fan combination, as shown in Fig. 1. This model uses a pulse-width modulated fan, 92 mm diameter, that is wired to run on maximum speed at all times (2,000 RPM) and has a rated power consumption of 2.64 W. The dimensions of the heatsink are 95 × 98 × 70 mm (W x L x H). The heatsink has 33 straight fins, a fin spacing of 1.6 mm at the base, fin thickness of 0.75 mm, and fin height of 35 mm. The Peltier element used for this study is rated at 12 V, 5.8 A, and has dimensions of 40 × 40 × 3.8 mm. Thermal paste, a 99.9% pure micronized silver paste designed to fill any gaps in the contact area between components, is used to provide a highly conductive bridge between the heatsink and Peltier element. The Peltier element is connected to a 13.8 V, 10 A DC power supply, and draws about 3 A when air-cooled. The heatsink fan is wired in parallel with the element.

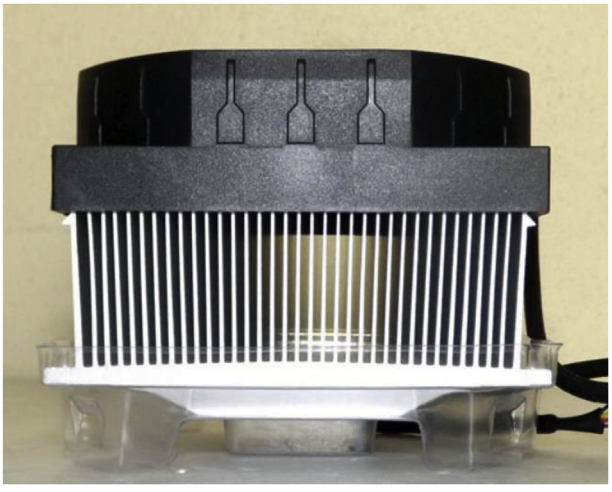

**Fig. 1.** Heatsink and fan combination used for the heat rejecting side of Peltier element—hot side heatsink.

Four different surface configurations were used for the water condensate collection measurement experiments. Each was connected to the Peltier element's cold side:

1. Plane aluminum plate: dimensions of 270 mm × 141 mm and a thickness of 3.18 mm.
2. Polytetrafluoroethylene (PTFE) coated plane aluminum plate: dimensions of 270 mm × 141 mm and a thickness of 3.00 mm.
3. Fanned aluminum plate: 101.6 mm wide, bottom plate 1 mm thick, top plate 0.65 mm thick, see Fig. 2 for other dimensions.
4. Aluminum heatsink, 76.75 × 76.75 × 69 mm (L x W x H), fin height 64 mm, 13 fins having a base thickness of 1.25 mm and tip thickness of 0.75 mm, 2 fins on each side with a base thickness of 2.25 mm and tip thickness of 1.50 mm; spacing between fins at base is 4 mm. See Fig. 3 for a schematic of the thermoelectric cooler (TEC) assembly.

The water condensate collection surfaces were placed facing an ultrasonic humidifier. The humidifier is set so that it provides enough moist air to simulate foggy conditions without condensation occurring on nearby non-cooled surfaces (near 100% relative humidity). Condensed water is drained into a collection container. At the end of each test, the temperature and humidity were measured, and the water in the collection container was transferred to a graduated cylinder and measured. The ambient temperature on the heat rejection side (hot heat sink) was controlled to be 19 °C ± 3 °C for all experiments. The water collected is compared to the consumed power measured using a watt meter to find the water per energy. The measurement uncertainty values for all experiments and the devices used to measure each quantity are shown in Table 1 and Table 2.

## 3. Results

### 3.1. Surfaces comparison results and discussion

For this experiment, the surfaces tested were a plane aluminum plate, a PTFE coated plane aluminum plate, a fanned aluminum plate, and a finned aluminum heatsink. All surfaces are placed vertically and the moist air from the humidifier is directed horizontally at the surfaces. Fig. 4 shows the orientation of the finned aluminum heatsink.

For the aluminum plate and PTFE plate experiments the surface is wiped clear with a rubber wiper every hour, denoted as “cleared” hereafter. Tests where the surface is left untouched are denoted as “uncleared.” Table 3 and Fig. 5 show the average collection rate of the tested surfaces in L/kWh. Fig. 6 shows a comparison of the surface areas of the different surface configurations investigated.

Fig. 5 shows a steady increase in the collection rates across the tested surfaces. The increase from the aluminum plate, to the fanned plate, to the heatsink as the surface areas increase is to be expected. However, when compared to Fig. 6, the collection rates do not increase at the same rate as the surface areas. This shows that the sizing of the heatsink seems to be appropriate for the used Peltier element being used. This is supported by the visual observation of the aluminum plate, PTFE plate, and fanned plate experiments, where the condensation occurred around the center of the Peltier element, and waned towards the edges of the collection surface.

The PTFE plate shows a 28%/30% (uncleared/cleared) higher collection rate than the aluminum plate, despite having the same surface area. The hydrophobic PTFE coating causes the condensate to bead up much more than on the aluminum plate, resulting in more dropwise condensation. A comparison of the surfaces during condensation is shown below in Fig. 7. Clearing the surfaces of the PTFE and aluminum plates results in a 16% increase in collection rate for the aluminum plate

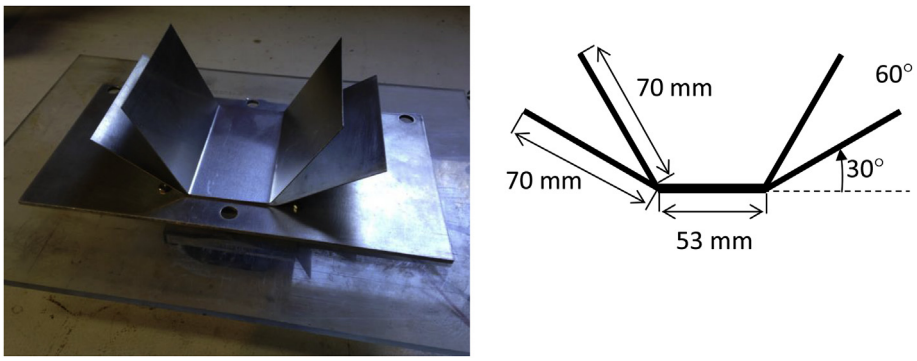


**Fig. 2.** Fanned aluminum plate.

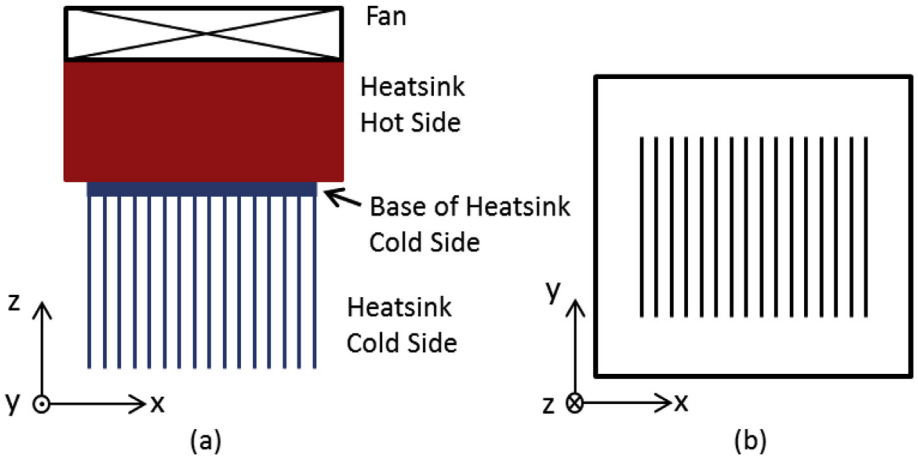


**Fig. 3.** (a) Schematic of assembly of TEC with aluminum heatsinks on hot and cold side (b) View on to cold side heatsink (bottom view - schematic).

**Table 1**
Measuring devices and uncertainties.

| | RH (%) | | T (°C) | H2O (ml) | H2O (L) | kWh |
|---|---|---|---|---|---|---|
| Uncertainty | <90%<br>>90% | ±2.50%<br>±5.00% | ±1 | ±5 | ±0.005 | ±0.005 |
| Measuring Device | Temperature Humidity Meter | | | Graduated Cylinder | | Watt Meter |

**Table 2**
Measuring devices and uncertainties for the tilted heatsink, tilted surface, and tilted heatsink timeline experiments.

| | Angle (°) | T (°C) | Ts (°C) | H2O (ml) | kWh | Interval (s) |
|---|---|---|---|---|---|---|
| Uncertainty | ±2 | ±1 | ±1 | ±5 | ±0.005 | 1 |
| Measuring Device | Protractor and Level | Thermometer | | Graduated Cylinder | Watt Meter | |

and 18% for the PTFE plate.

### 3.2. Rotated and tilted heatsink experiments

The objective of the presented experiments is to determine the effect of the fin orientation on the water collection rate. Two orientations with seven different angles each have been investigated as shown in Fig. 8 and Fig. 9.

### 3.3. Rotated heatsink results and discussion

The average collection rates for the different angles tested in the rotated heatsink experiment are presented in Table 4 and Fig. 10.

The results in Fig. 10 show a maximum collection rate for the rotated heatsink at an angle of 60°. This is unexpected because one might assume that a vertical fin arrangement (0°) results in the best drainage of condensed water because gravity assists the drainage of water from the fins. For the given heatsink, a vertical orientation is found to be the worst in terms of water collection rate. Starting at 45°, condensate bridging between fins is observed. The amount of water bridging between fins increases as the angle increases. At 90° (horizontal), the entire space between fins eventually fills with water. This is shown in Figs. 11, 12, 13, and 14.

Note that Fig. 10 has two columns for the 90° angle, one with a 9-hour test duration and one with a 24-hour test duration. The 9-hour test has a much higher collection rate because during the test the heatsink never reached maximum capacity (when the spaces between the fins are completely filled), and all of the water collected during the test was held by the heatsink for the entire test duration. In other words, nearly all the water collected was collected at the end of the test when the heatsink was drained for measuring. The 24-hour test has a lower collection rate because the heatsink did reach maximum capacity at the 10-hour mark when it started collecting at approximately 0.026 L/kWh. Still, the vast majority of the water was collected by draining the heatsink at the end of the test. This shows that the horizontal orientation is highly inefficient over long periods of time, but effective over the short periods, assuming the condensate is then removed. More importantly, it suggests that reaching capacity, or too much bridging, is detrimental to the collection rate.

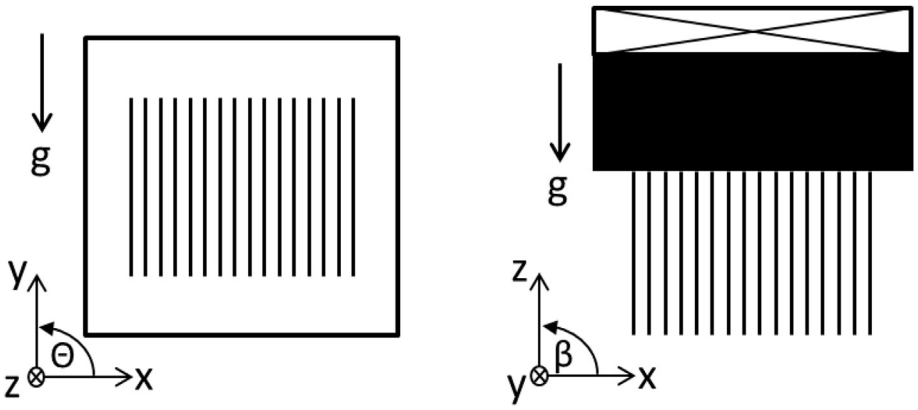


**Fig. 4.** Orientation of heatsink for surfaces comparison experiments; g denotes the action of gravity; Θ is the rotation angle; β is the tilting angle.

**Table 3**
Average Collection rates for uncleared and cleared experiments of surfaces: aluminum plate, PTFE plate, fanned plate, and heatsink.

| Aluminum Plate | Average L/kWh | Uncertainty (±L/kWh) |
|---|---|---|
| Uncleared | 0.058 | 0.009 |
| Cleared | 0.067 | 0.012 |
| PTFE Plate | | |
| Uncleared | 0.074 | 0.006 |
| Cleared | 0.087 | 0.009 |
| Fanned Plate | | |
| Uncleared | 0.103 | 0.013 |
| Heatsink | | |
| Uncleared | 0.123 | 0.009 |

### 3.4. Tilted heatsink results and discussion

The average collection rates for the different angles tested in the tilted heatsink experiment are presented in Table 5 and Fig. 15.

The maximum collection rate for the tilted heatsink occurs at an angle of 75°. The trend—increasing collection rate with increasing angle—is similar to the rotated heatsink results. For angles of 0°, 15°, and 30° the collection rates differ by less than 3% between the rotated and tilted heatsink experiments. Slightly higher values for the collection rate are observed for the rotated heatsink at 45°, 60° and 75°, but only the collection rate at 60° shows a difference of more than 10%, 19% higher for the rotated case. Condensate bridging between fins was observed to start at 60° (Fig. 16), increasing in severity as the tilt angle increases (Fig. 17). At 90° (horizontal), all but a small passage through the center of the heatsink fills, restricting the airflow through the heatsink, until eventually the passage filled up as well, which the 24 h test showed (Fig. 18).

The 24-hour test of the tilted heatsink at 90° confirmed what was observed for the rotated heatsink experiment at 90°. The collection rates are identical within the measurement uncertainty (less than 3% difference) and this is expected since the physical orientation between both experiments is the same.

### 3.5. Flat plate tilted heatsink results and discussion

The purpose of the flat plate tilted experiment is to determine the effect of surface orientation on a single-side collection surface in isolation. The results are then compared to the tilted heatsink experiments to determine if the results observed are simply a combination of the effects of an upward and downward facing surface, or if some other effect, such as bridging, has any significant impact. The polytetrafluoroethylene (PTFE) coated plane aluminum plate was used. Fig. 19 shows the orientation of the flat plate at angles of 15° and 165°.

The surface is tilted such that the condensation surface is upward facing at a 15° angle from the horizontal, and then rotated down in 15° increments for each test until an angle of 165° is reached. Angles closer to the horizontal, 0°–15°, are omitted for this experiment due to difficulties managing accurate condensate collection. Angles from 165° to 180° are also omitted because the condensate no longer runs down the pan surface consistently, and instead drips from the pan over a wide area. Table 6 and Fig. 20 show the average collection rates for the different angles tested in

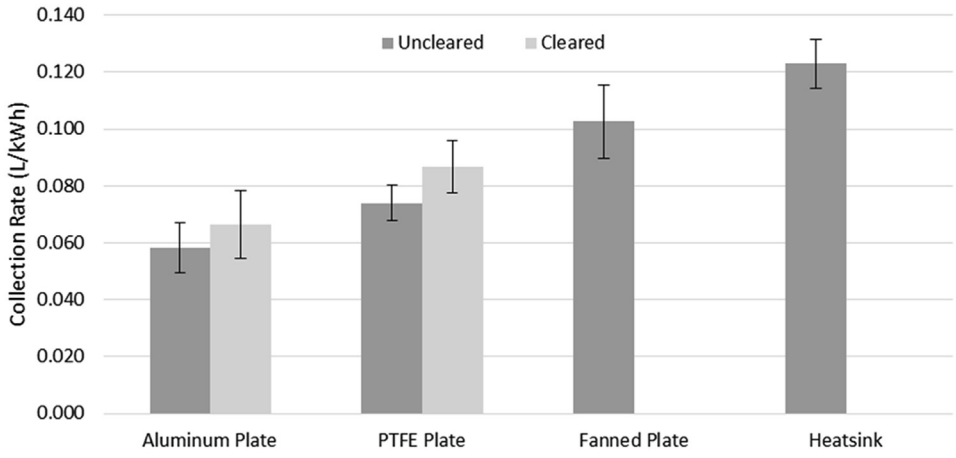


**Fig. 5.** Average Collection rates for uncleared and cleared experiments of surfaces: aluminum plate, PTFE plate, fanned plate, and heatsink.

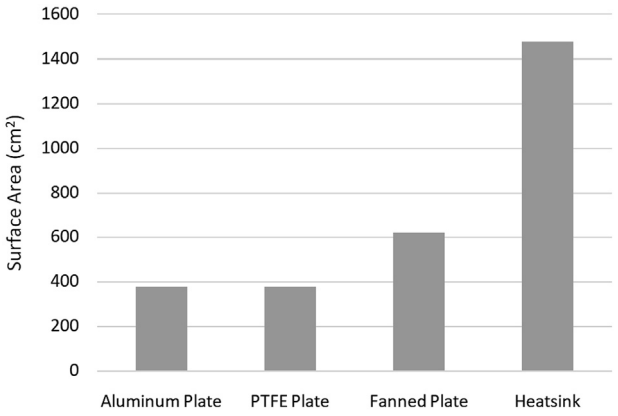


**Fig. 6.** Comparison of surface areas.

this experiment.

As shown in Fig. 20, the data has a maximum water collection rate occurring at 15° and steadily declining to a minimum water collection rate at 165°. The decline as a function of tilt angle can be explained by the flow that is created by a cold natural convection surface. While the surface is tilted upward, the cold humid air wants to cling to the surface, providing more time for condensation, while when it is tilted down, the cold humid air wants to fall away from the surface.

Fig. 21 compares the results from the tilted heatsink experiment to the results of the tilted surface angles combined to create the same angle as the heatsink. For example, the 30° tilt on the heatsink (with each fin having two sides) is paired with a combination of the 60° and 120° angles—two single sides representing the upward and downward facing sides of the heatsink fin. Because of the difference in surface area, the water collection rates are represented as a percentage increase from the collection rate at the vertical position for each respective experiment. For the tilted surface experiment, the two angles' percent increases were individually calculated, then averaged to find an estimated combined effect to compare to the double-sided fin of the heatsink.

The results show a difference in percent increase, but a similar trend between the tilted heatsink and flat surface combination between 0° and 45°, suggesting that the surface combination is a reasonable approximation of the fin for these angles. At 60° the percent difference between

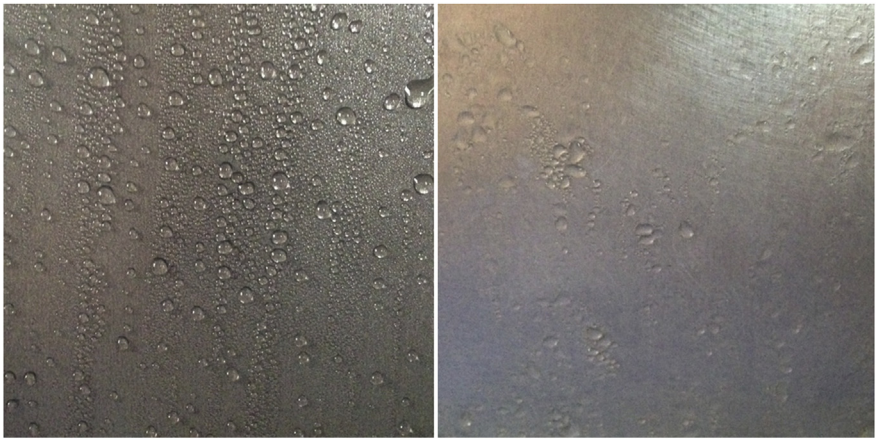

**Fig. 7.** PTFE plate (left) and aluminum plate (right) surface comparison during condensation.

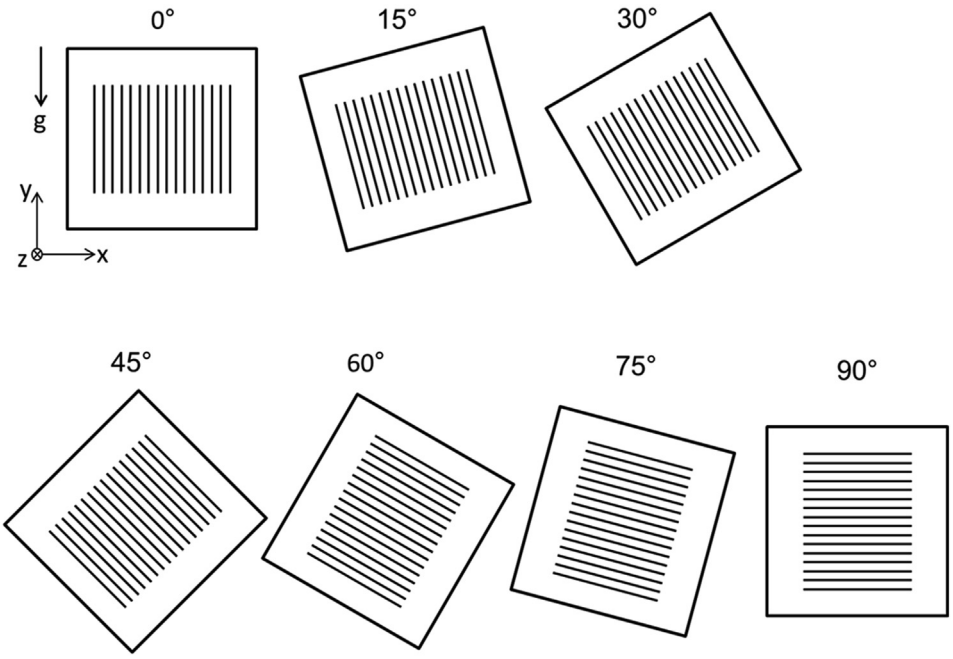


**Fig. 8.** Rotated heatsink experiments.

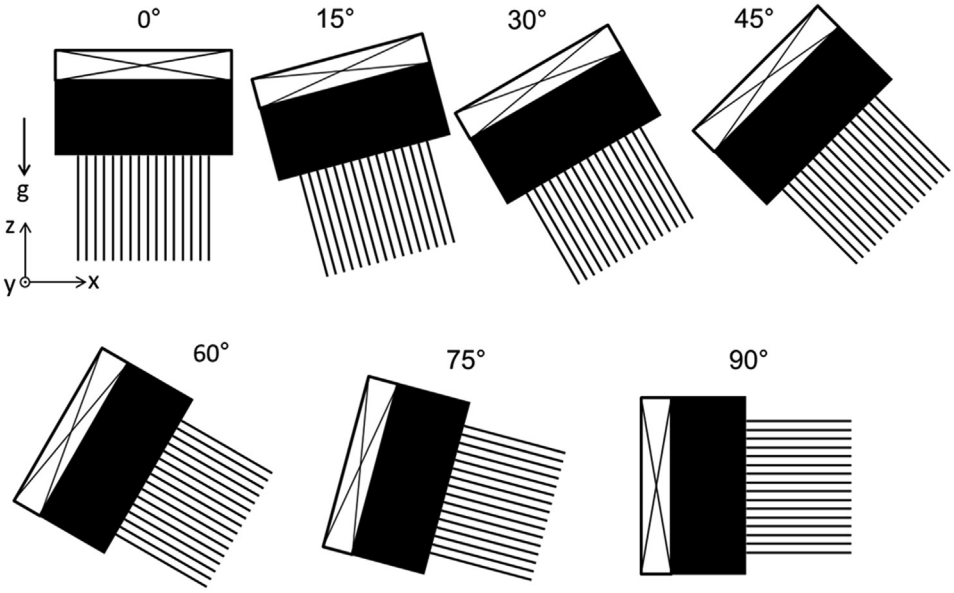


**Fig. 9.** Tilted heatsink experiments.

**Table 4**
Average collection rates for the rotated heatsink experiments.

| Angle (°) | Average L/kWh | Uncertainty (±L/kWh) | Average kWh/m$^3$ | Uncertainty (±kWh/m$^3$) |
|---|---|---|---|---|
| 0 | 0.132 | 0.018 | 7577 | 1026 |
| 15 | 0.157 | 0.018 | 6364 | 724 |
| 30 | 0.177 | 0.018 | 5652 | 571 |
| 45 | 0.213 | 0.018 | 4696 | 394 |
| 60 | 0.249 | 0.018 | 4020 | 289 |
| 75 | 0.234 | 0.018 | 4280 | 327 |
| 90 (9 h) | 0.203 | 0.018 | 4938 | 436 |
| 90 (24 h) | 0.127 | 0.018 | 7879 | 1110 |

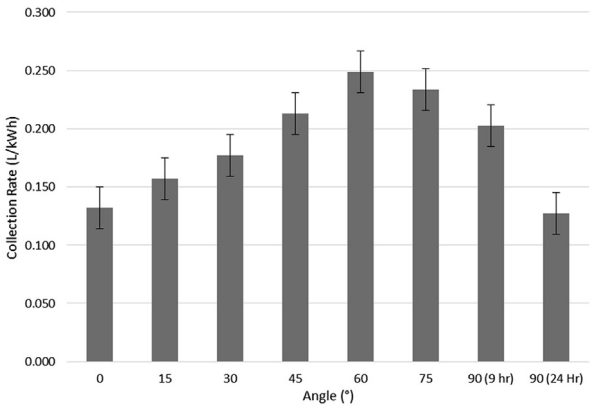


**Fig. 10.** Average collection rates for the rotated heatsink experiments.

the two increases. At 60° condensate bridging between the fins started to occur in the tilted heatsink experiment, which cannot occur in the tilted surface experiment. At 75°, the difference is less, possibly indicating that bridging has less of an effect on the water collection rate at this angle. These results lend credence to the hypothesis that some amount of bridging increases the water collection rate presented in the tilted heatsink results. However, the evidence is not conclusive based on the given experimental data and further research into the effect of bridging is necessary.

**Fig. 11.** Rotated heatsink at 45° angle.

It should be noted that the combined surface representation is an approximation of the heatsink fin. A possible reason for the discrepancy between the heatsink and surface combination values shown is that the heatsink fins share one source of heat transfer between both sides of the fin, while the combined surfaces each have one source. Meaning that for the combined surfaces, each side removes an equal amount of heat.

## 4. Conclusion

Based on the conducted surface experiments at a vertical orientation, the PTFE coated plate showed up to a 30% higher water collection rate

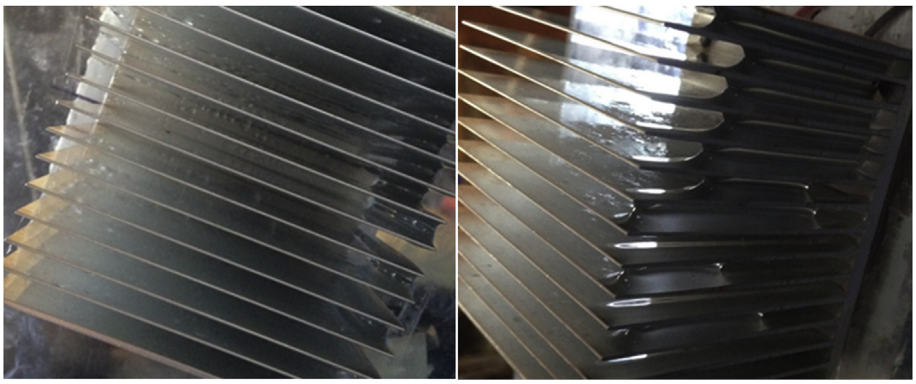

**Fig. 12.** Rotated heatsink at 60° angle.

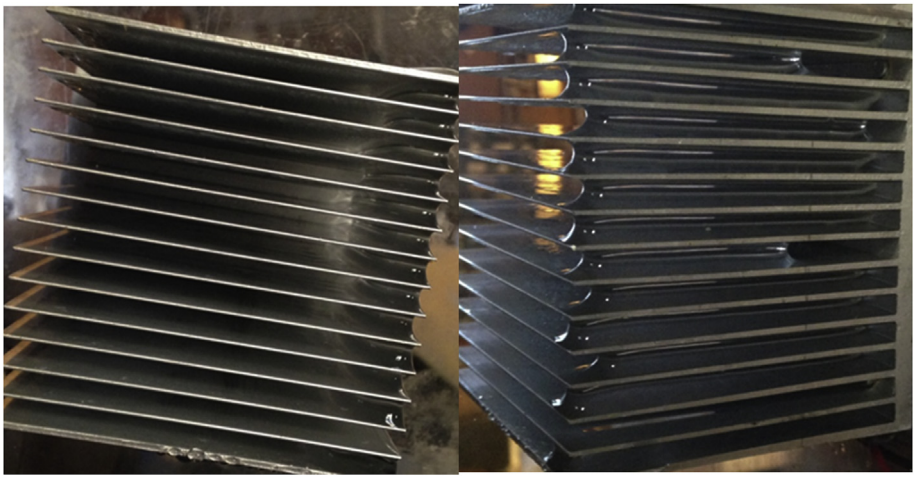

**Fig. 13.** Rotated heatsink at 75° angle.

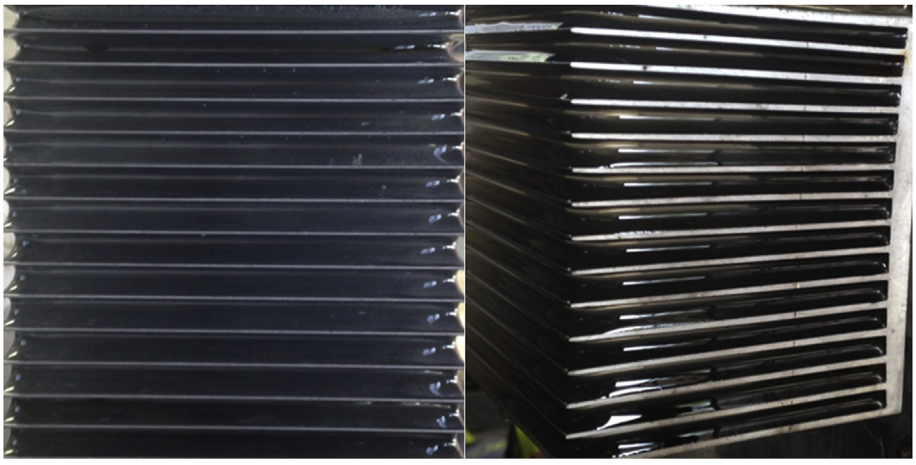

**Fig. 14.** Rotated heatsink at 90° angle.

compared to the uncoated flat plate having the same surface area because of improved dropwise condensation as a result of the hydrophobic surface. Clearing the surfaces—i.e., removing all condensate every hour—increased the water collection rate up to 18% for the flat plates. Increasing the surface area by 64% using the fanned plate increases the collection rate by 78% compared to the uncoated flat plate (uncleared). The finned heatsink has a 288% larger surface area than the flat plates and the collection rate increased by 112% compared to the uncoated flat plate (uncleared) and 66% compared to the PTFE coated flat plate (uncleared).

The finned heatsink and the PTFE coated flat plate were used for the orientation experiments. The finned heatsink was rotated from 0° to 90° as well as tilted from 0° to 90° (vertical to horizontal). The maximum collection rate for the rotated heatsink is found at an angle of 60°. Starting at a minimum of 45° condensate bridging between fins was observed. The amount of water bridging between fins increases as the angle increases. At 90° (horizontal), the entire space between fins eventually fills with water. The two extended time experiments show that once the spaces between the fins are filled with water the water collection rate drops significantly—by an order of magnitude, from 0.203 L/

**Table 5**
Average collection rates for the tilted heatsink experiments.

| Angle (°) | Average L/kWh | Uncertainty (±L/kWh) | Average kWh/m$^3$ | Uncertainty (±kWh/m$^3$) |
|---|---|---|---|---|
| 0 | 0.135 | 0.018 | 7429 | 987 |
| 15 | 0.155 | 0.018 | 6471 | 748 |
| 30 | 0.180 | 0.018 | 5561 | 553 |
| 45 | 0.195 | 0.018 | 5122 | 469 |
| 60 | 0.210 | 0.018 | 4755 | 404 |
| 75 | 0.221 | 0.018 | 4519 | 365 |
| 90 (24 h) | 0.130 | 0.018 | 7709 | 1062 |

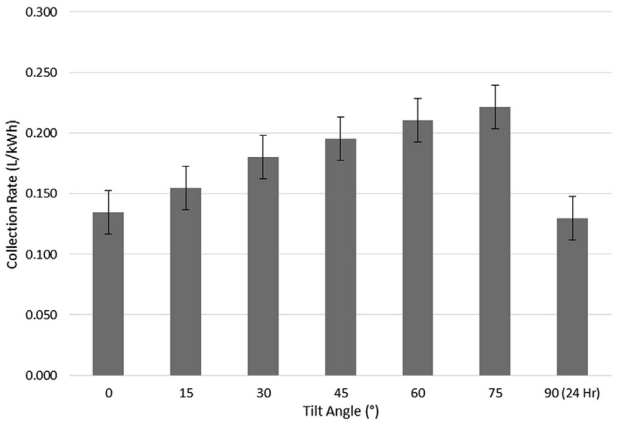


**Fig. 15.** Average collection rates for the heatsink tilted at 0°, 15°, 30°, 45°, 60°, 75°, and 90°.

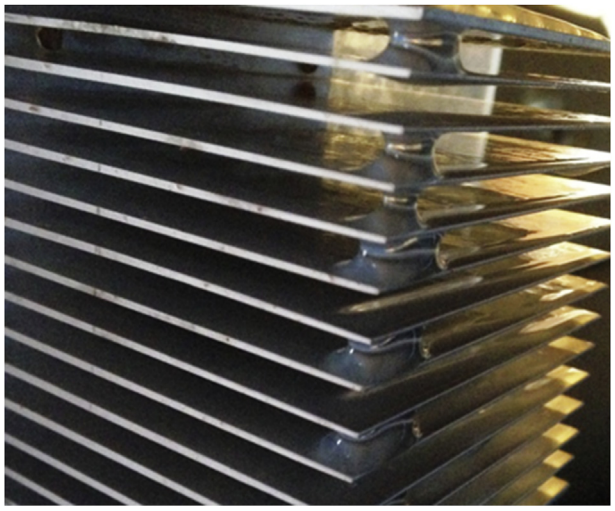

**Fig. 16.** Tilted heatsink condensate bridging at 60°.

kWh to 0.026 L/kWh. This result indicates that the horizontal orientation is highly inefficient over long periods of time.

The maximum water collection rate for the tilted heatsink is found at an angle of 75°. The trend—increasing collection rate with increasing angle—is similar to the rotated heatsink results. For angles of 0°, 15°, and 30° the water collection rates differ by less than 3% between the rotated and tilted heatsink experiments. Slightly higher values for the water collection rate are observed for the rotated heatsink at 45°, 60° and 75°, but only the water collection rate at 60° shows a difference of more than 10%–19%. Condensate bridging between fins was observed to start at 60° and the amount of water bridging between fins increases as the angle increases. At 90° (horizontal), the entire space between fins eventually fills with water confirming the results of the rotated heatsink at 90° since

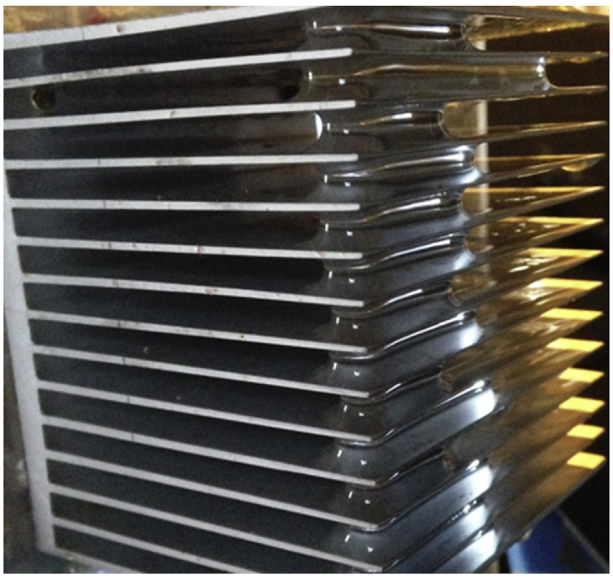

**Fig. 17.** Tilted heatsink condensate bridging at 75°.

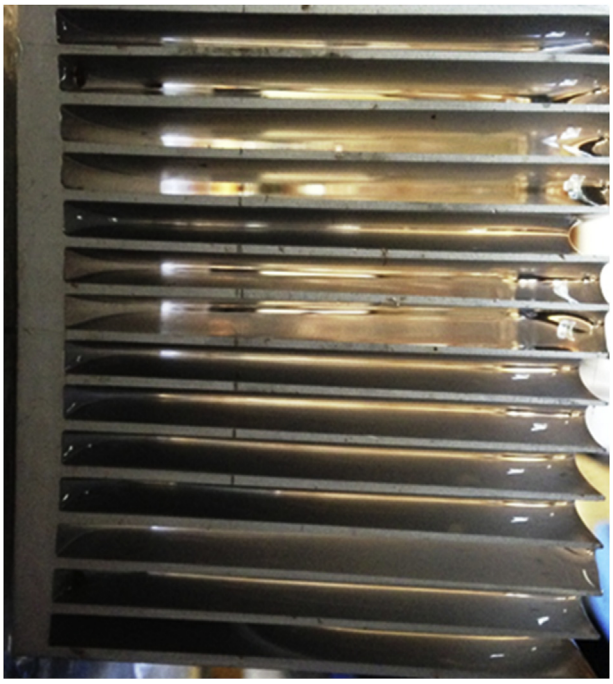

**Fig. 18.** Tilted heatsink condensate bridging at 90° after 24 h.

the two orientations are identical.

The PTFE coated flat plate tilted experiments confirm the trend observed from the tilted heatsink between 0° and 45° showing an increase in collection rate with increase in tilt angle. However, at 60° there is a departure between the two because condensate bridging between the fins started to occur in the tilted heatsink experiment. Given that the tilted surface experiment does not experience bridging, the difference between the two experiments indicate that some amount of bridging increases the water collection rate presented in the tilted heatsink results.

It should be noted that the objective of this study was to investigate the effect of heatsink orientation on water condensate collection rate and therefore the absolute values reported in this study do not necessarily indicate the highest achievable values, i.e. with further optimization the absolute values will most likely be higher.

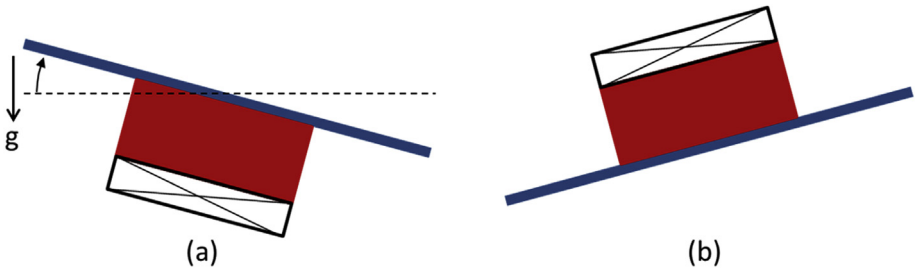


**Fig. 19.** Orientation of flat plate tilted heatsink experiments: (a) Angle of 15°, (b) Angle of 165°.

**Table 6**
Average collection rates for the flat plate PTFE surface tilted from 15° to 165° in 15° intervals.

| Angle (°) | Average L/kWh | Uncertainty (±) | Average kWh/m$^3$ | Uncertainty (±) |
|---|---|---|---|---|
| 15 | 0.319 | 0.012 | 3134 | 113 |
| 30 | 0.239 | 0.012 | 4192 | 202 |
| 45 | 0.213 | 0.012 | 4704 | 255 |
| 60 | 0.180 | 0.012 | 5562 | 356 |
| 75 | 0.136 | 0.012 | 7339 | 620 |
| 90 | 0.125 | 0.012 | 7972 | 732 |
| 105 | 0.110 | 0.012 | 9110 | 955 |
| 120 | 0.100 | 0.012 | 10024 | 1157 |
| 135 | 0.100 | 0.012 | 9958 | 1141 |
| 150 | 0.071 | 0.012 | 13988 | 2252 |
| 165 | 0.055 | 0.012 | 18217 | 3820 |

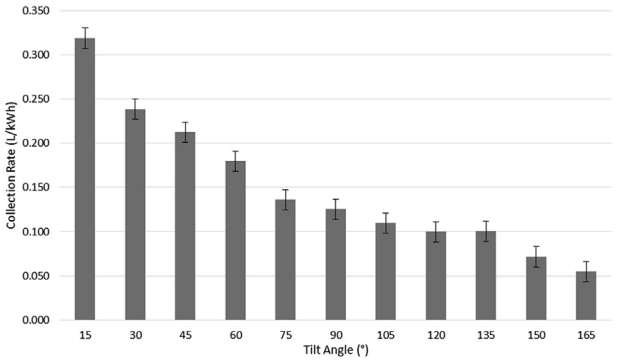


**Fig. 20.** Average collection rates for the flat plate PTFE surface tilted from 15° to 165° in 15° intervals.

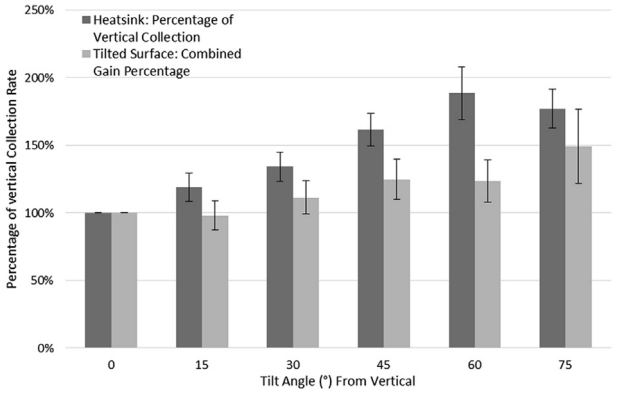


**Fig. 21.** Percentage of vertical collection of the tilted heatsink and associated combined angles of the tilted surface experiments, from 0° to 75° from the vertical.

Future research should consider the orientation of heatsinks as well as surface coating when trying to optimize thermoelectric cooling for atmospheric water condensation.

## Declarations

### *Author contribution statement*

Carson T. Hand: Conceived and designed the experiments; Performed the experiments; Analyzed and interpreted the data; Contributed reagents, materials, analysis tools or data; Wrote the paper.

Steffen Peuker: Conceived and designed the experiments; Analyzed and interpreted the data; Contributed reagents, materials, analysis tools or data; Wrote the paper.

### *Funding statement*

This work was supported by Cal Poly Heating, Ventilation, Air-Conditioning and Refrigeration Industrial Advisory Board.

### *Competing interest statement*

The authors declare no conflict of interest.

### *Additional information*

No additional information is available for this paper.

## References

[1] Y.A. Çengel, A.J. Ghajar, Heat and Mass Transfer : Fundamentals & Applications, sixth ed., McGraw-Hill, New York, 2020.
[2] M. Singh, N.D. Pawar, S. Kondaraju, S.S. Bahga, Modeling and simulation of dropwise condensation: a review, J. Indian Inst. Sci. 99 (2019) 157–171.
[3] M.-H. Kim, C.W. Bullard, Air-side performance of brazed aluminum heat exchangers under dehumidifying conditions, Int. J. Refrig. 25 (2002) 924–934.
[4] C. Korte, A.M. Jacobi, Condensate retention effects on the performance of plain-fin-and-tube heat exchangers: retention data and modeling, J. Heat Transf. 123 (2001) 926.
[5] M. Edalatpour, L. Liu, A.M. Jacobi, K.F. Eid, A.D. Sommers, Managing water on heat transfer surfaces: a critical review of techniques to modify surface wettability for applications with condensation or evaporation, Appl. Energy 222 (2018) 967–992.
[6] D. Milani, A. Abbas, A. Vassallo, M. Chiesa, D. Al Bakri, Evaluation of using thermoelectric coolers in a dehumidification system to generate freshwater from ambient air, Chem. Eng. Sci. 66 (2011) 2491–2501.
[7] S. Liu, W. He, D. Hu, S. Lv, D. Chen, X. Wu, F. Xu, S. Li, Experimental analysis of a portable atmospheric water generator by thermoelectric cooling method, Energy Procedia 142 (2017) 1609–1614.
[8] J.G. Vián, D. Astrain, M. Domínguez, Numerical modelling and a design of a thermoelectric dehumidifier, Appl. Therm. Eng. 22 (2002) 407–422.
[9] V.P. Joshi, V.S. Joshi, H.A. Kothari, M.D. Mahajan, M.B. Chaudhari, K.D. Sant, Experimental investigations on a portable fresh water generator using a thermoelectric cooler, Energy Procedia 109 (2017) 161–166.

[10] M.A. Muñoz-García, G.P. Moreda, M.P. Raga-Arroyo, O. Marín-González, Water harvesting for young trees using Peltier modules powered by photovoltaic solar energy, Comput. Electron. Agric. 93 (2013) 60–67.
[11] M. Eslami, F. Tajeddini, N. Etaati, Thermal analysis and optimization of a system for water harvesting from humid air using thermoelectric coolers, Energy Convers. Manag. 174 (2018) 417–429.
[12] F. Tan, S.C. Fok, Experimental testing and evaluation of parameters on the extraction of water from air using thermoelectric coolers, J. Test. Eval. 41 (2013) 96–103.